Pathways to excitation of atoms with bicircular laser pulses

J. Venzke, Y. Gebre, A. Becker, and A. Jaroń-Becker
Joint Institute for Laboratory Astrophysics and Department of Physics, University of Colorado, Boulder, Colorado 80309-0440, USA

(Received 19 February 2020; revised manuscript received 7 April 2020; accepted 16 April 2020; published 14 May 2020; corrected 25 August 2020)

We study the excitation of the hydrogen atom by bichromatic circularly polarized laser pulses using numerical solutions of the time-dependent Schrödinger equation. The results are in agreement with the selection rules for multiphoton processes in such fields, namely, excited states are populated in which orbital angular momentum and magnetic quantum numbers are either both odd or both even, independent of the relative helicity, peak intensity, and pulse duration of the pulses. For co-rotating pulses the results show that excitation predominantly proceeds to states with magnetic quantum number of the same helicity as the laser pulses. Besides pathways via direct photon absorption from the ground state our results indicate that a transfer of population among the Rydberg states occurs via Λ-type transitions. In the case of counter-rotating pulses the largest excitation probability is found for Rydberg states that differ in magnetic quantum number by $\Delta m = \pm 3$. This pattern allows us to estimate how many photons from each of the two bichromatic fields have been absorbed. Finally, we confirm that a population in Rydberg states beyond a maximum orbital angular quantum number is unlikely.

DOI: 10.1103/PhysRevA.101.053425

I. INTRODUCTION

Recently, studies on the interaction of atoms and molecules with intense fields generated by the superposition of two circularly polarized laser pulses have seen an upsurge in activity in strong-field experiment and theory. For the most part, the renewed interest results from the capability to control the polarization of emitted light in high-order harmonic generation with such pulses. The physical principle has been proposed and applied first two decades ago [1,2]. More recently, efficient phase matching of circularly polarized high-order harmonic beams in the EUV and soft-x-ray regime using bichromatic beams with counter-rotating circular polarization has been demonstrated [3–7]. Since then, much experimental and theoretical work on high-harmonic generation [8–32], ionization and photoelectron momentum distributions [33–53], double ionization [54–60], and other strong-field processes [61–63] driven by bichromatic circularly polarized laser pulses has been performed. One interesting aspect in these kinds of strong-field interactions is the control of ionization via the helicity of the applied bichromatic pulses [35,36,49]. Such studies complement related work on the dependence of the ionization rate by a one-color circularly pulse on the relative helicity between the pulse and the electron in the atomic orbital [64–78].

For bichromatic circularly polarized laser pulses it has been observed that the probability to ionize an atom is significantly enhanced if the two fields are counter-rotating as compared to co-rotating fields [36]. The experimental observations were interpreted as due to the increased density of excited states accessible for resonant enhanced multiphoton ionization in the case of counter-rotating fields. Results of numerical solutions of the time-dependent Schrödinger equation in Ref. [36] did confirm a close relation between the ratios of total excitation and ionization probabilities for counter-rotating and co-rotating circularly polarized laser pulses. However, the results for excitation of the atom were not further resolved by distributions over the quantum numbers (principal, angular momentum, magnetic). Such analysis potentially can shed further light on the role of excited states in the pathways to ionization since excitation in a resonant multiphoton process should rely on the spin angular momentum selection rules for the absorption of circularly polarized photons ($\Delta l = \pm 1$ and $\Delta m = \pm 1$).

More generally, analysis of the role of strong-field excitation has recently experienced a renaissance [79–82] following earlier work [83–85]. Concerning the distribution in the excited states with respect to the quantum numbers only studies for the interaction of atoms with linearly polarized pulses have been performed. Theoretical studies have considered the distribution of the population as a function of the principal and/or the angular momentum quantum number [86–91]. In applications of Floquet theory for a monochromatic laser field [86] and numerical calculations for laser pulses with trapezoidal [90] and Gaussian or sin-squared envelopes [91] it has been analyzed how the parity of the populated angular momentum states in such pulses relates to the selection rules for linearly polarized pulses. In view of the recent experimental observations discussed above, we extend these studies to interaction of atoms with bichromatic circularly polarized laser pulses. Such study provides the interesting opportunity not only to resolve the excited-state distribution with respect to the principal or angular orbital momentum quantum number but in particular to consider the role of the magnetic quantum number as well. For our studies we make use of results of numerical solutions of the time-dependent Schrödinger equation for the interaction of the hydrogen atom with intense bichromatic circularly polarized laser pulses.

The paper is organized as follows. In Sec. II we briefly summarize the standard methods used to solve the

time-dependent Schrödinger equation for the interaction of the hydrogen atom with bicircular laser pulses. The results of the numerical calculations are then presented and analyzed in Sec. III, first for co-rotating and then for counter-rotating pulses. In Sec. IV we summarize the insights gained into the excitation pathways in bicircular pulses.

II. NUMERICAL METHOD

The time-dependent Schrödinger equation for the interaction of an electron in the potential of the hydrogen atom with a superposition of two circularly polarized intense laser pulses in dipole approximation and velocity gauge is given by (we use Hartree atomic units $e = m_e = \hbar = 1$)

$$i\frac{\partial}{\partial t}\Psi(\mathbf{r},t) = \left[-\frac{\nabla^2}{2} - \frac{-i\mathbf{A}(t)\cdot\nabla}{c} - \frac{1}{r}\right]\Psi(\mathbf{r},t), \quad (1)$$

where $\mathbf{A}(t)$ is the vector potential of the two laser pulses. The wave function Ψ is expanded in spherical harmonics up to $l_{\max} = 45$ and $m_{\max} = 45$. The radius is discretized using fourth-order finite difference method with a grid spacing of 0.1 a.u. and a maximum radius of 750 a.u. with exterior complex scaling on the outer 38 a.u. of the grid. The wave function is propagated in time using the Crank-Nicolson method with a time step of 0.05 a.u. The choice of gauge was based on the faster convergence of calculations in the velocity gauge for expansions of the wave function in spherical harmonics [92,93].

The interaction with the bicircular laser pulse is implemented via the total vector potential as

$$\mathbf{A}(t) = \mathbf{A}_\omega(t) + \mathbf{A}_{2\omega}(t) \quad (2)$$

where

$$\mathbf{A}_\Omega(t) = A_{0,\Omega}\sin^2\left(\frac{\pi t}{\tau_\Omega}\right) \times [\sin(\Omega t)\hat{\mathbf{x}} + \epsilon_\Omega\cos(\Omega t)\hat{\mathbf{y}}] \quad (3)$$

for $\Omega = \omega$ and 2ω, respectively. $A_{0,\Omega} = \frac{c\sqrt{I_\Omega}}{\Omega}$, $\tau_\Omega = \frac{2\pi N_\Omega}{\Omega}$, and c is the speed of light, where I_Ω is the peak intensity and N_Ω denotes the number of cycles. $\epsilon_\Omega = \pm 1$ denotes the helicity of the fundamental and second-harmonic pulse, respectively.

We have performed numerical calculations for the interaction of the hydrogen atom with co- and counter-rotating bicircular pulses operating at the central wavelengths of 800 and 400 nm. Intensities of the two pulses were varied to study the distribution in the excited states as a function of all quantum numbers—principal, angular momentum, and magnetic. For the results presented below we have used pulses with the same pulse duration in time.

III. RESULTS

In this section we present the results for the distributions, first for the co-rotating and then for the counter-rotating case, which provide insights into selection rules and excitation pathways in bichromatic multiphoton processes.

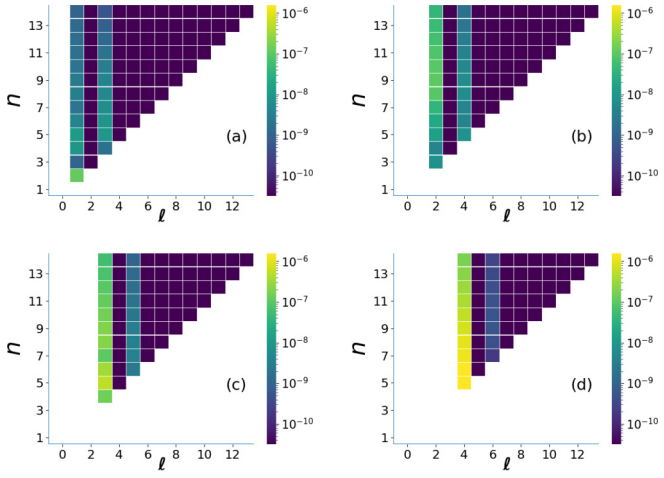

FIG. 1. Excited-state distribution as a function of n (vertical axis) and ℓ (horizontal axis) for (a) $m = -1$, (b) $m = -2$, (c) $m = -3$, and (d) $m = -4$ at the end of 20 (at 800-nm) cycle pulses (40 cycles at 400 nm) with sin squared envelope and total peak intensity of 1×10^{14} W/cm^2 for co-rotating laser pulses of equal intensity.

A. Excitation with co-rotating pulses

Selection rules for (single-)photon absorption from circularly polarized light are given by $\Delta l = \pm 1$ and $\Delta m = \pm 1$, where the change in the magnetic quantum number is positive (negative) if the helicity of the light is right (left) handed. Extending the concept to multiphoton absorption, the simultaneous change in both quantum numbers puts distinct constraints on the parity and helicity of the accessible excited states in the atoms upon absorption of multiple photons. Specifically, it is expected that states in which ℓ and m are either both even or both odd are being populated during the interaction with the field. This selection holds for the interaction with a single circularly polarized pulse as well as for the case of a superposition of two (or more) of such fields, independent of the relative helicity of the two pulses.

In Fig. 1 we show examples of the population in the excited states of the hydrogen atom as a function of n and ℓ for various m values at the end of the interaction with bichromatic co-rotating left-handed circularly polarized pulses. The results clearly confirm the expected population distribution in states with either odd or even parity for a given value of m according to the selection rules upon multiphoton absorption. The present results have been obtained for interaction with equal peak intensities $I_{400} = I_{800} = 5 \times 10^{13}$ W/cm^2.

Due to the correlation in changes of m and ℓ the observed pattern is independent of total peak intensity, ratio of peak intensities, and pulse duration, as long as the dipole approximation holds. In the present paper we have verified this up to intensities of 1×10^{14} W/cm^2. This is different from the case of linear polarization [91], where selective population concerning the parity of the populated excited states is observed for long pulses and low peak intensities only. In that case the restriction to a given m channel and a broad energy spectrum (for short pulse durations) or a significant Stark shift of the excited states (at high peak intensities) leads to a mixing of population over the states with odd and even orbital angular momentum quantum numbers.

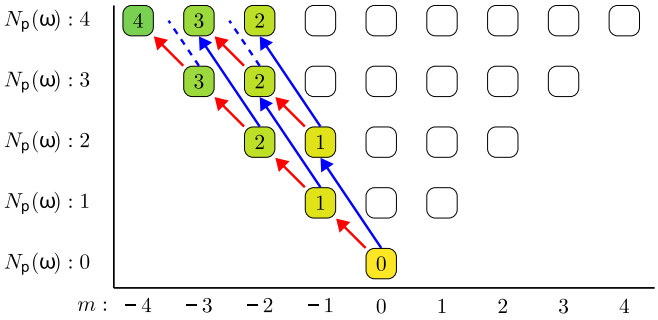

FIG. 2. Absorption pathways in co-rotating laser pulses at frequencies ω and 2ω starting from a $m = 0$ state. Without lack of generalization it is assumed that both pulses have left-handed helicity. Absorption of a photon at frequency ω and at frequency 2ω is represented by a red and blue arrow, respectively. The numbers in the boxes denote the minimum number of photons to reach a certain level.

In co-rotating bicircular laser pulses all the photons have the same spin (either $+1$ or -1), consequently the magnetic quantum number always changes either by $\Delta m = +1$ or by $\Delta m = -1$ upon absorption of each photon. For our studies we have chosen left-handed helicity for both pulses and, hence, only excited states with negative m can be populated upon absorption of photons from the ground state with $m = 0$ (see Fig. 2). Therefore, as already mentioned in Ref. [38], only Rydberg states with high orbital angular quantum number ℓ are accessible. For example, for excitation of Rydberg states (with $n \geqslant 4$) in the hydrogen atom, the absorption of at least four photons in the laser field at 400 nm or at least eight photons at 800 nm is required. Thus, Rydberg states with $\ell < 4$ (and $m > -4$) cannot be populated via photon absorption alone.

Accordingly, the angular momentum distribution in the Rydberg states is controlled via the relative intensity of the two fields at the fundamental and second-harmonic frequency. This is demonstrated in Fig. 3, where the excited-state distribution as a function of ℓ, summed for $n \geqslant 4$ and all m, is shown. For large ratio of $I_{400}/I_{800} = 10$ [panel (a)] the distribution is centered, as expected, about $\ell = 4$. As the intensity ratio decreases, high orbital angular momentum states get increasingly populated due to the impact of the laser pulse at 800 nm.

Another interesting feature in Fig. 3 is that the population in angular momentum states with $\ell < 4$ increases significantly when the intensities of the two pulses are similar. Further insight can be gained by the distribution over the magnetic quantum number, which is displayed in Fig. 4(c) for the case of equal intensities. It is clearly seen that Rydberg states with magnetic quantum numbers between $m = 0$ and -3 are populated. In view of the number of photons needed to reach the Rydberg levels, the population in these states cannot be explained by absorption of photons only.

Instead, we propose the following mechanism: Initially, Rydberg states with $\ell \geqslant 4$ are populated via the absorption pathways shown in Fig. 2. Then a redistribution of population occurs via Raman-type Λ transitions (see Refs. [94,95]). In the present bichromatic laser field the Λ process leads to a

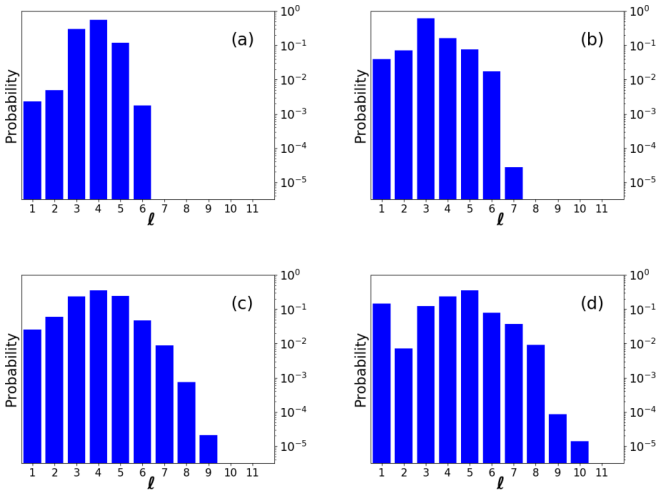

FIG. 3. Normalized excited-state distribution as a function of orbital angular quantum number ℓ summed over $n \geqslant 4$ and m at (a) $I_{400} = 5 \times 10^{13}\,\mathrm{W/cm^2}$, $I_{800} = 5 \times 10^{12}\,\mathrm{W/cm^2}$; (b) $I_{400} = 5 \times 10^{13}\,\mathrm{W/cm^2}$, $I_{800} = 1 \times 10^{13}\,\mathrm{W/cm^2}$; (c) $I_{400} = 5 \times 10^{13}\,\mathrm{W/cm^2}$, $I_{800} = 5 \times 10^{13}\,\mathrm{W/cm^2}$; and (d) $I_{400} = 1 \times 10^{13}\,\mathrm{W/cm^2}$, $I_{800} = 5 \times 10^{13}\,\mathrm{W/cm^2}$. Pulse durations: 20 cycles at 400 nm, ten cycles at 800 nm.

change in the magnetic quantum number, if photons from both fields are involved. For the absorption of one 400-nm photon and emission of two 800-nm photons the magnetic quantum number between initial and final state changes by $\Delta m = +1$.

The order of absorption and emission may vary, i.e., the redistribution process can proceed either via the continuum [absorption first, Fig. 4(a)] or via a lower excited state [emission first, Fig. 4(b)]. A larger change in m is achieved either via a sequence of these Λ processes or by higher-order processes (e.g., absorption of two 400-nm photons followed by emission of four 800-nm photons leading to $\Delta m = +2$). We note that similarly the absorption of two photons at 800 nm and the emission of a 400-nm photon will lead to a change of $\Delta m = -1$ in the present setup and, hence, contribute to population of states with higher ℓ and m.

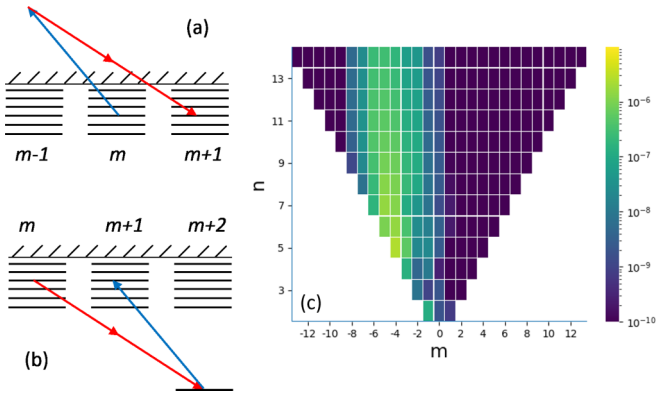

FIG. 4. Excited-state distribution as a function of n (vertical axis) and m (horizontal axis) summed over ℓ. Laser parameters: 20 (800-nm) cycle pulses with sin squared envelope and total peak intensity of $1 \times 10^{14}\,\mathrm{W/cm^2}$ for co-rotating laser pulses of equal intensity.

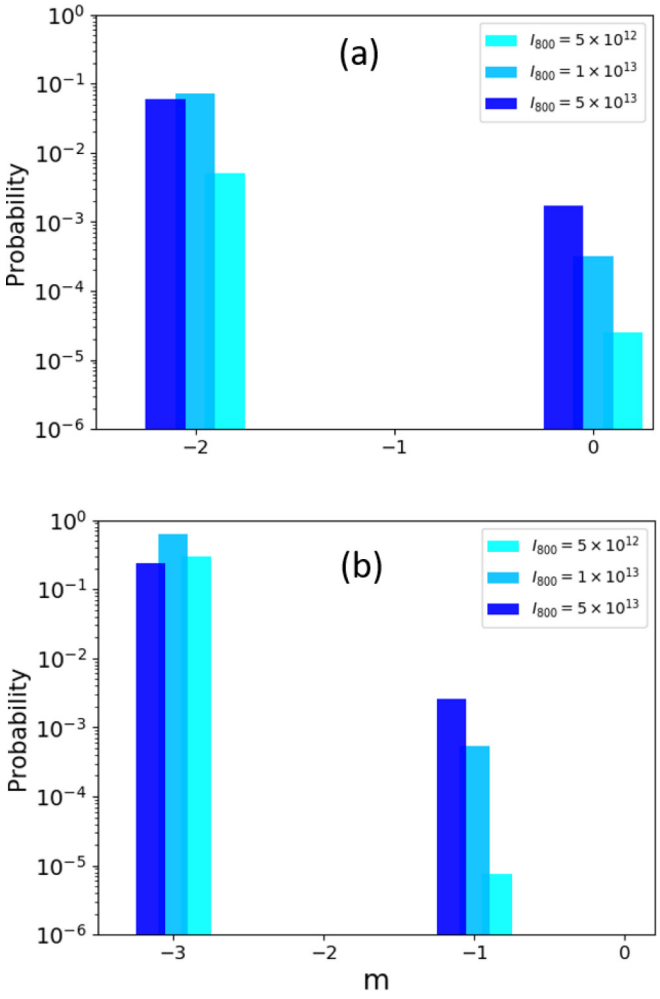

FIG. 5. Normalized distribution in magnetic quantum states for (a) $\ell = 2$ and (b) $\ell = 3$ and different peak intensities of the 800-nm pulse. $I_{400} = 5 \times 10^{13}\,\mathrm{W/cm^2}$ and other parameters are as in Fig. 4.

Our interpretation is further supported by the results in Fig. 5, which shows how the population in states of certain quantum numbers for (a) $\ell = 2$ and (b) $\ell = 3$ changes as a function of the relative intensity of the two pulses. It is clearly seen that the population in these quantum states, which are not accessible via direct absorption of photons from the ground state, increases as the intensity of the pulse at 800 nm increases. Thus, these results provide further indications that the presence of the redistribution process depends on the impact of both pulses and its effectiveness increases with increase of the total intensity, in agreement with our interpretation of a Λ-type process.

B. Excitation with counter-rotating pulses

As discussed in the previous subsection, the selection rules state that only states with ℓ and m either both even or both odd hold independent of the relative helicity of the two pulses. This is confirmed by the results that we obtained for the interaction with two counter-rotating pulses at equal intensities and equal pulse duration presented in Fig. 6. Depending on whether m is even or odd, the distribution over the orbital

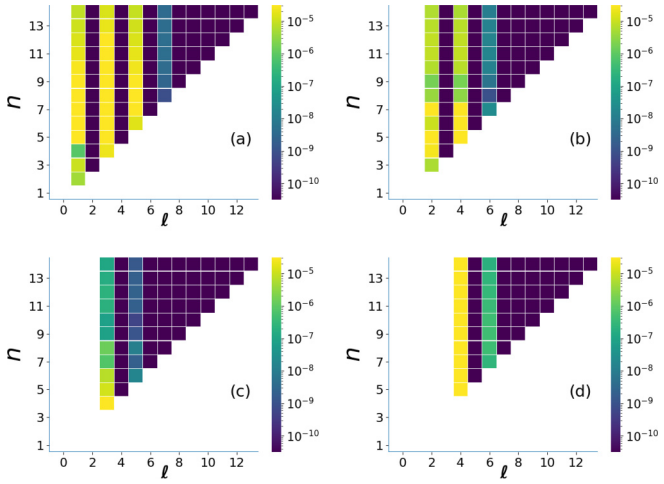

FIG. 6. Same as Fig. 1 but for counter-rotating laser pulses.

angular momentum shows population in states with even or odd parity. As in the case of co-rotating pulses, the observed pattern is found independent of total peak intensity, ratio of peak intensities, and pulse duration.

Since in counter-rotating bicircular laser pulses photons of the two fields have opposite spin, starting from the ground state with $m = 0$, excited states with both positive and negative magnetic quantum numbers can be populated. The absorption pathways for the setup chosen in the present paper, namely, right-handed helicity for the 800-nm pulse and left-handed helicity for the second harmonic, are shown in Fig. 7. As can be seen from the figure, the magnetic quantum number reflects the difference between the numbers of 400- and 800-nm photons that are absorbed. Furthermore, it can be seen that for a given total photon energy absorbed states with magnetic quantum numbers separated by $\Delta m = \pm 3$ are populated.

These features are clearly present in the population distributions as a function of m, summed over n and ℓ (top), and of n and m, summed over ℓ (bottom), in Fig. 8, which show the results for counter-rotating pulses of equal peak intensity. In the Rydberg manifold ($n \geqslant 4$) the highest populated m states differ by $\Delta m = \pm 3$, and other states show some but lower population as the manifold is ac Stark shifted during

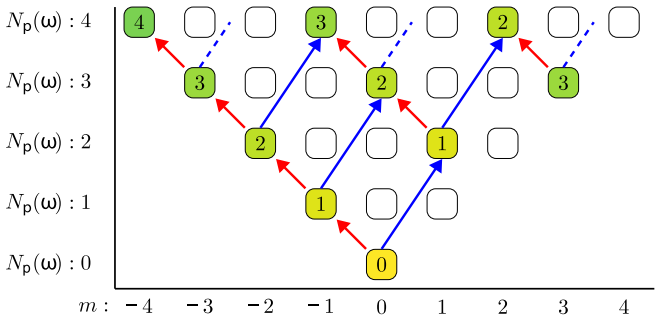

FIG. 7. Absorption pathways in counter-rotating laser pulses at frequencies ω and 2ω starting from a $m = 0$ state. Without lack of generalization it is assumed that the pulse at frequency ω has left-handed helicity, while the second-harmonic pulse has right-handed velocity. Other symbols are as in Fig. 2.

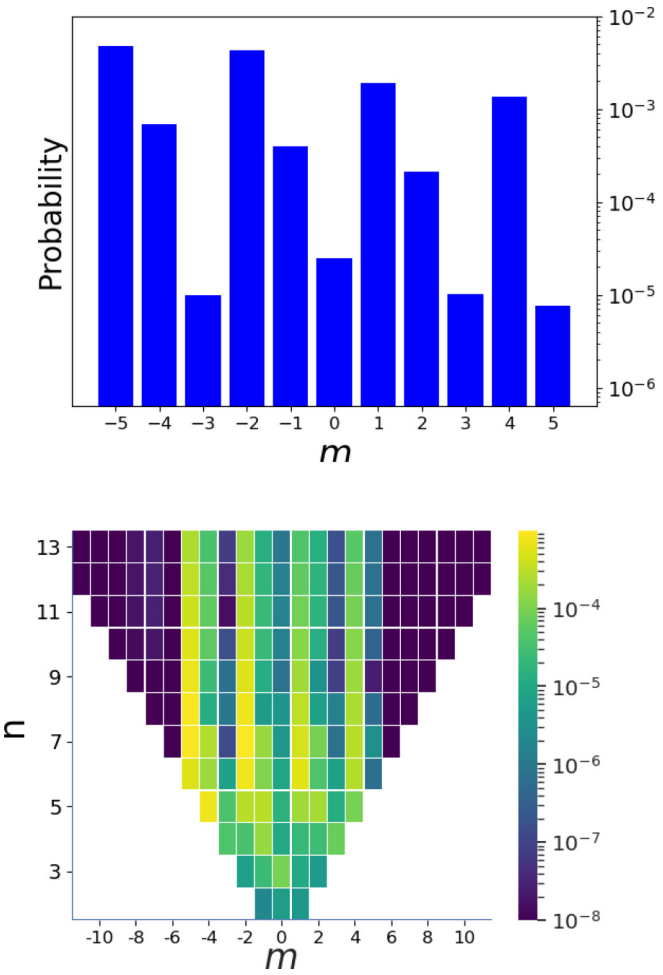

FIG. 8. Excited-state distributions as a function of m, summed over $n \geqslant 4$ and ℓ (top), and as a function of n and m, summed over ℓ (bottom), for the interaction with a left-handed circularly polarized laser pulse at 800 nm (20 cycles) and a right-handed circularly polarized laser pulse at 400 nm (40 cycles). Both pulses have the same peak intensity of 5×10^{13} W/cm^2.

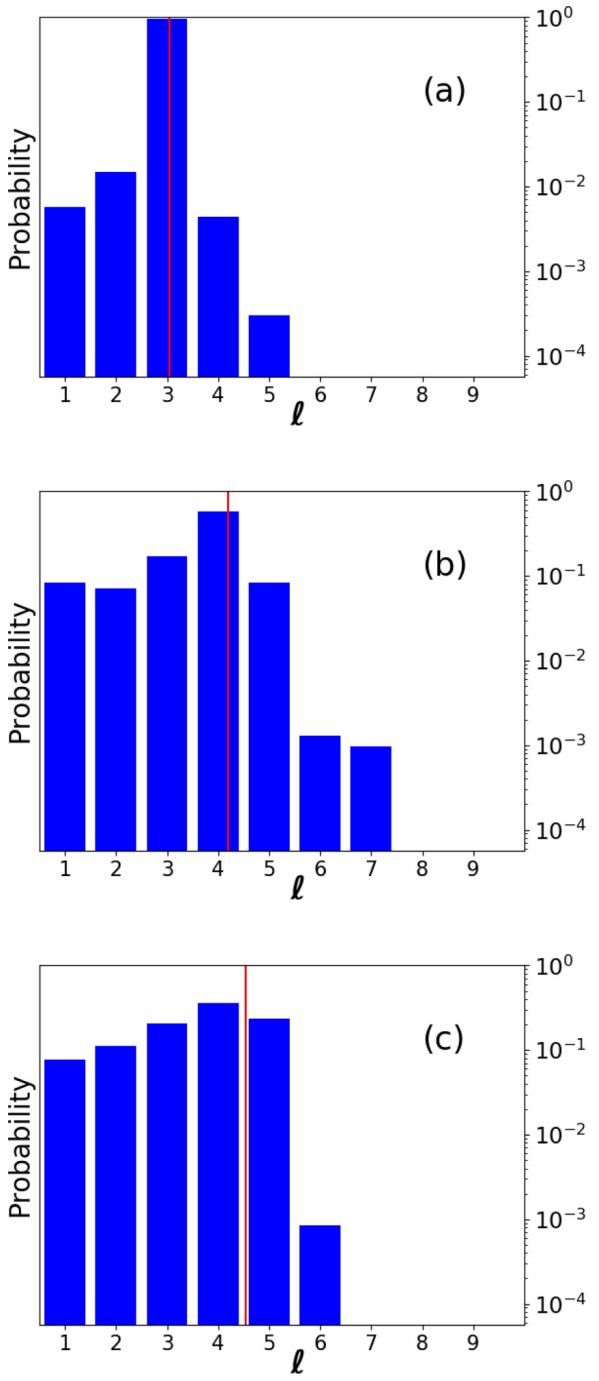

FIG. 9. Normalized orbital angular momentum distributions in excited states induced by counter-rotating laser pulses at 400 nm (20 cycles) and 800 nm (ten cycles) at peak intensities of (a) $I_{400} = 5 \times 10^{13}$ W/cm^2, $I_{800} = 5 \times 10^{12}$ W/cm^2; (b) $I_{400} = 5 \times 10^{12}$ W/cm^2, $I_{800} = 5 \times 10^{13}$ W/cm^2; and (c) $I_{400} = 5 \times 10^{13}$ W/cm^2, $I_{800} = 5 \times 10^{13}$ W/cm^2.

the interaction with the pulses. In view of the nonlinearity of multiphoton processes, it is likely that the states showing the largest probability are being populated near the peak of the pulses at which the highest total intensity is present. Overall, the strongest population is seen for states with negative magnetic quantum numbers, leading to the conclusion that it is most likely that either five (for excited states with $m = -5$) or two (for excited states with $m = -2$) more 800-nm photons with left-handed helicity than 400-nm photons with right-handed helicity are being absorbed.

The distributions in Fig. 8 do not extend much beyond $|m| = 5$, which is consistent with the results shown in Fig. 9, showing that there appears to be a highest orbital angular momentum number $\ell_{\max}$ beyond which the population in the states drops off quickly. This is in agreement with previous studies for Rydberg state excitation [90,91] and low-energy angular momentum distributions [96]. In Ref. [96] a random-walk analysis of the absorption pathways between the accessible quantum states is used to obtain the classical orbital angular momentum for an electron with zero energy in a laser field derived as $L = \sqrt{2Z\alpha_0}$ where Z is the charge of the residual ion and α_0 is the quiver radius. Relating classical orbital angular momentum and the orbital angular momentum quantum number by $\ell \approx L - 1/2$ we have estimated the maximum ℓ gained in the bicircular counter-rotating pulse. The estimates, shown by the solid red lines in Fig. 9, are in

good agreement with the cutoffs seen in the numerical results. We note that the random-walk analysis of Ref. [96] can be applied in the case of counter-rotating pulses, since in each absorption step $\Delta m = \pm 1$ and hence, in general, $\Delta \ell = \pm 1$ is possible. In contrast, for co-rotating pulses the changes in magnetic and angular quantum number are determined in each absorption step ($\Delta m = -1$, $\Delta \ell = +1$) and hence a random-walk analysis is not applicable and a cutoff cannot be derived.

IV. SUMMARY

We have studied the distributions over the orbital angular momentum (ℓ) and magnetic (m) quantum numbers in Rydberg states due to the interaction with bichromatic circularly polarized laser pulses. Multiphoton selection rules lead to population of states in which ℓ and m are either both even or both odd, independent of relative helicity, peak intensity, and pulse duration. In the case of co-rotating pulses the results show that the distribution over the magnetic quantum number can be controlled via the intensities of the two pulses. Furthermore, we propose that the states are populated via direct absorption from the ground state and via Λ-type transitions between Rydberg states of different ℓ and m, involving two photons at the fundamental wavelength and one photon at the second harmonic. For bicircular laser pulses with opposite helicities Rydberg states with magnetic quantum numbers that differ by $\Delta m = \pm 3$ are predominantly populated. The pattern allows us to gain insights into the relative number of photons absorbed from the two fields. The distribution is, however, restricted by the maximum orbital angular momentum quantum number that can be estimated by classical considerations.

ACKNOWLEDGMENTS

This work was primarily supported (J.V., Y.G., A.B.) by a grant from the US Department of Energy, Division of Chemical Sciences, Atomic, Molecular, and Optical Sciences Program (Grant No. DE-SC0001771). A.J.-B. acknowledges support by a grant from the US National Science Foundation (Grant No. PHY-1734006).

J.V. and Y.G. contributed equally to this work.

[1] H. Eichmann, A. Egbert, S. Nolte, C. Momma, B. Wellegehausen, W. Becker, S. Long, and J. K. McIver, Phys. Rev. A **51**, R3414 (1995).
[2] S. Long, W. Becker, and J. K. McIver, Phys. Rev. A **52**, 2262 (1995).
[3] A. Fleischer, O. Kfir, T. Diskin, P. Sidorenko, and O. Cohen, Nat. Photon. **8**, 543 (2014).
[4] E. Pisanty, S. Sukiasyan, and M. Ivanov, Phys. Rev. A **90**, 043829 (2014).
[5] O. Kfir, P. Grychtol, E. Turgut, R. Knut, D. Zusin, D. Popmintchev, T. Popmintchev, H. Nembach, J. M. Shaw, A. Fleischer, H. Kapteyn, M. Murnane, and O. Cohen, Nat. Photon. **9**, 99 (2015).
[6] T. Fan, P. Grychtol, R. Knut, C. Hernandez-Garcia, D. D. Hickstein, D. Zusin, C. Gentry, F. J. Dollar, C. A. Mancuso, C. W. Hogle, O. Kfir, D. Legut, K. Carva, J. L. Ellis, K. M. Dorney, C. Chen, O. G. Shpyrko, E. E. Fullerton, O. Cohen, P. M. Oppeneer, D. B. Milosevic, A. Becker, A. Jaron-Becker, T. Popmintchev, M. M. Murnane, and H. C. Kapteyn, Proc. Natl. Acad. Sci. USA **112**, 14206 (2015).
[7] D. D. Hickstein, F. J. Dollar, P. Grychtol, J. Ellis, R. Knut, C. Hernandez-Garcia, D. Zusin, C. Gentry, J. Shaw, T. Fan, K. Dorney, A. Becker, A. Jaron-Becker, H. C. Kapteyn, and M. M. Murnane, Nat. Photon. **9**, 743 (2015).
[8] D. B. Milosevic, J. Phys. B **48**, 171001 (2015).
[9] L. Medisauskas, J. Wragg, H. van der Hart, and M. Y. Ivanov, Phys. Rev. Lett. **115**, 153001 (2015).
[10] D. B. Milosevic, Opt. Lett. **40**, 2381 (2015).
[11] C. Chen, Z. Tao, C. Hernandez-Garcia, P. Matyba, A. Carr, R. Knut, O. Kfir, D. Zusin, C. Gentry, P. Grychtol, O. Cohen, L. Plaja, A. Becker, A. Jaron-Becker, H. Kapteyn, and M. Murnane, Sci. Adv. **2**, e1501333 (2016).
[12] D. Baykusheva, M. S. Ahsan, N. Lin, and H. J. Wörner, Phys. Rev. Lett. **116**, 123001 (2016).
[13] C. Hernandez-Garcia, C. G. Durfee, D. D. Hickstein, T. Popmintchev, A. Meier, M. M. Murnane, H. C. Kapteyn, I. J. Sola, A. Jaron-Becker, and A. Becker, Phys. Rev. A **93**, 043855 (2016).
[14] X. Liu, X. Zhu, L. Li, Y. Li, Q. Zhang, P. Lan, and P. Lu, Phys. Rev. A **94**, 033410 (2016).
[15] F. Mauger, A. D. Bandrauk, and T. Uzer, J. Phys. B **49**, 10LT01 (2016).
[16] A. D. Bandrauk, F. Mauger, and K. J. Yuan, J. Phys. B **49**, 23LT01 (2016).
[17] D. M. Reich and L. B. Madsen, Phys. Rev. Lett. **117**, 133902 (2016).
[18] S. Odzak, E. Hasovic, and D. B. Milosevic, Phys. Rev. A **94**, 033419 (2016).
[19] K. M. Dorney, J. L. Ellis, C. Hernandez-Garcia, D. D. Hickstein, C. A. Mancuso, N. Brooks, T. Fan, G. Fan, D. Zusin, C. Gentry, P. Grychtol, H. C. Kapteyn, and M. M. Murnane, Phys. Rev. Lett. **119**, 063201 (2017).
[20] A. Fleischer, E. Bordo, O. Kfir, P. Sidorenko, and O. Cohen, J. Phys. B **50**, 034001 (2017).
[21] N. Zhavoronkov and M. Ivanov, Opt. Lett. **42**, 4720 (2017).
[22] E. Pisanty and A. Jimenez-Galan, Phys. Rev. A **96**, 063401 (2017).
[23] D. Baykusheva, S. Brennecke, M. Lein, and H. J. Wörner, Phys. Rev. Lett. **119**, 203201 (2017).
[24] G. Lerner, T. Diskin, O. Neufeld, O. Kfir, and O. Cohen, Opt. Lett. **42**, 1349 (2017).
[25] D. Ayuso, P. Decleva, S. Patchkovskii, and O. Smirnova, J. Phys. B **51**, 06LT01 (2018).
[26] G. Dixit, A. Jimenez-Galan, L. Medisauskas, and M. Ivanov, Phys. Rev. A **98**, 053402 (2018).
[27] L. Barreau, K. Veyrinas, V. Gruson, S. J. Weber, T. Auguste, J.-F. Hergott, F. Lepetit, B. Carre, J.-C. Houver, D. Dowek, and P. Salieres, Nat. Commun. **9**, 4727 (2018).

[28] P.-C. Huang, C. Hernandez-Garcia, J.-T. Huang, P.-Y. Huang, C.-H. Lu, L. Rego, D. D. Hickstein, J. L. Ellis, A. Jaron-Becker, A. Becker, S.-D. Yang, C. G. Durfee, L. Plaja, H. C. Kapteyn, M. M. Murnane, A. H. Kung, and M.-C. Chen, Nat. Photon. **12**, 349 (2018).

[29] A. Jimenez-Galan, N. Zhavoronkov, D. Ayuso, F. Morales, S. Patchkovskii, M. Schloz, E. Pisanty, O. Smirnova, and M. Ivanov, Phys. Rev. A **97**, 023409 (2018).

[30] J. Heslar, D. A. Telnov, and Shih-I Chu, Phys. Rev. A **97**, 043419 (2018).

[31] W. Paufler, B. Böning, and S. Fritzsche, Phys. Rev. A **98**, 011401(R) (2018).

[32] M.-Z. Li, Y. Xu, G.-R. Jia, and X.-B. Bian, Phys. Rev. A **100**, 033410 (2019).

[33] J. M. Ngoko Djiokap, S. X. Hu, L. B. Madsen, N. L. Manakov, A. V. Meremianin, and A. F. Starace, Phys. Rev. Lett. **115**, 113004 (2015).

[34] K. J. Yuan, S. Chelkowski, and A. D. Bandrauk, Phys. Rev. A **93**, 053425 (2016).

[35] D. B. Milosevic, Phys. Rev. A **93**, 051402(R) (2016).

[36] C. A. Mancuso, D. D. Hickstein, K. M. Dorney, J. L. Ellis, E. Hasovic, R. Knut, P. Grychtol, C. Gentry, M. Gopalakrishnan, D. Zusin, F. J. Dollar, X.-M. Tong, D. B. Milosevic, W. Becker, H. C. Kapteyn, and M. M. Murnane, Phys. Rev. A **93**, 053406 (2016).

[37] D. B. Milosevic and W. Becker, Phys. Rev. A **93**, 063418 (2016).

[38] C. A. Mancuso, K. M. Dorney, D. D. Hickstein, J. L. Chaloupka, X.-M. Tong, J. L. Ellis, H. C. Kapteyn, and M. M. Murnane, Phys. Rev. A **96**, 023402 (2017).

[39] D. Pengel, S. Kerbstadt, D. Johannmeyer, L. Englert, T. Bayer, and M. Wollenhaupt, Phys. Rev. Lett. **118**, 053003 (2017).

[40] M. Busuladzic, A. Gazibegovic-Busuladzic, and D. B. Milosevic, Phys. Rev. A **95**, 033411 (2017).

[41] V.-H. Hoang, V.-H. Le, C. D. Lin, and A.-T. Le, Phys. Rev. A **95**, 031402(R) (2017).

[42] K. Lin, X. Jia, Z. Yu, F. He, J. Ma, H. Li, X. Gong, Q. Song, Q. Ji, W. Zhang, H. Li, P. Lu, H. Zeng, J. Chen, and J. Wu, Phys. Rev. Lett. **119**, 203202 (2017).

[43] M. Abu-samha and L. B. Madsen, J. Phys. B **51**, 135401 (2018).

[44] M. Busuladzic, A. Cerkic, A. Gazibegovic-Busuladzic, E. Hasovic, and D. B. Milosevic, Phys. Rev. A **98**, 013413 (2018).

[45] S. Eckart, M. Kunitski, I. Ivanov, M. Richter, K. Fehre, A. Hartung, J. Rist, K. Henrichs, D. Trabert, N. Schlott, L. Ph. H. Schmidt, T. Jahnke, M. S. Schöffler, A. Kheifets, and R. Dörner, Phys. Rev. A **97**, 041402(R) (2018).

[46] M. Li, W.-C. Jiang, H. Xie, S. Luo, Y. Zhou, and P. Lu, Phys. Rev. A **97**, 023415 (2018).

[47] M. Han, P. Ge, Y. Shao, Q. Gong, and Y. Liu, Phys. Rev. Lett. **120**, 073202 (2018).

[48] S. Eckart, K. Fehre, N. Eicke, A. Hartung, J. Rist, D. Trabert, N. Strenger, A. Pier, L. Ph.H. Schmidt, T. Jahnke, M. S. Schöffler, M. Lein, M. Kunitski, and R. Dörner, Phys. Rev. Lett. **121**, 163202 (2018).

[49] M.-M. Liu, Y. Shao, M. Han, P. Ge, Y. Deng, C. Wu, Q. Gong, and Y. Liu, Phys. Rev. Lett. **120**, 043201 (2018).

[50] N. Eicke and M. Lein, Phys. Rev. A **99**, 031402(R) (2019).

[51] P. Ge, M. Han, Y. Deng, Q. Gong, and Y. Liu, Phys. Rev. Lett. **122**, 013201 (2019).

[52] S. Kerbstadt, K. Eickhoff, T. Bayer, and M. Wollenhaupt, Nat. Commun. **10**, 658 (2019).

[53] M. Abu-samha and L. B. Madsen, Phys. Rev. A **100**, 043415 (2019).

[54] C. A. Mancuso, K. M. Dorney, D. D. Hickstein, J. L. Chaloupka, J. L. Ellis, F. J. Dollar, R. Knut, P. Grychtol, D. Zusin, C. Gentry, M. Gopalakrishnan, H. C. Kapteyn, and M. M. Murnane, Phys. Rev. Lett. **117**, 133201 (2016).

[55] S. Eckart, M. Richter, M. Kunitski, A. Hartung, J. Rist, K. Henrichs, N. Schlott, H. Kang, T. Bauer, H. Sann, L. Ph.H. Schmidt, M. Schöffler, T. Jahnke, and R. Dörner, Phys. Rev. Lett. **117**, 133202 (2016).

[56] S. Ben, P.-Y. Guo, X.-F. Pan, T.-T. Xu, K.-L. Song, and X.-S. Liu, Chem. Phys. Lett. **679**, 38 (2017).

[57] J. M. Ngoko Djiokap, A. V. Meremianin, N. L. Manakov, S. X. Hu, L. B. Madsen, and A. F. Starace, Phys. Rev. A **96**, 013405 (2017).

[58] W.-W. Yu, S. Ben, L. Yi, Y.-S. Liu, J. Guo, and X.-S. Liu, Chem. Phys. Lett. **706**, 62 (2018).

[59] C. Huang, M. Zhong, and Z. Wu, Opt. Express **26**, 26045 (2018).

[60] X. Ma, Y. Zhou, Y. Chen, M. Li, Y. Li, Q. Zhang, and P. Lu, Opt. Express **27**, 1825 (2019).

[61] K. J. Yuan and A. D. Bandrauk, Phys. Rev. A **92**, 063401 (2015).

[62] G. Buica, Phys. Rev. A **98**, 053427 (2018).

[63] J. Guo, K.-J. Yuan, H. Lu, and A. D. Bandrauk, Phys. Rev. A **99**, 053416 (2019).

[64] I. Barth and O. Smirnova, Phys. Rev. A **84**, 063415 (2011).

[65] A. K. Kazansky, A. V. Grigorieva, and N. M. Kabachnik, Phys. Rev. A **85**, 053409 (2012).

[66] T. Herath, L. Yan, S. K. Lee, and W. Li, Phys. Rev. Lett. **109**, 043004 (2012).

[67] I. Barth and O. Smirnova, Phys. Rev. A **87**, 013433 (2013).

[68] J. H. Bauer, F. Mota-Furtado, P. F. O'Mahony, B. Piraux, and K. Warda, Phys. Rev. A **90**, 063402 (2014).

[69] I. Barth and M. Lein, J. Phys. B **47**, 204016 (2014).

[70] C. H. Raymond Ooi, W. L. Ho, and A. D. Bandrauk, Phys. Rev. A **90**, 013417 (2014).

[71] A. Hartung, F. Morales, M. Kunitski, K. Henrichs, A. Laucke, M. Richter, T. Jahnke, A. Kalinin, M. Schöffler, L. Ph.H. Schmidt, M. Ivanov, O. Smirnova, and R. Dörner, Nat. Photon. **10**, 526 (2016).

[72] N. Douguet, A. N. Grum-Grzhimailo, E. V. Gryzlova, E. I. Staroselskaya, J. Venzke, and K. Bartschat, Phys. Rev. A **93**, 033402 (2016).

[73] J. Wätzel and J. Berakdar, Phys. Rev. A **94**, 033414 (2016).

[74] J.-P. Wang and F. He, Phys. Rev. A **95**, 043420 (2017).

[75] Q. Zhang, G. Basnayake, A. Winney, Y. F. Lin, D. Debrah, S. K. Lee, and W. Li, Phys. Rev. A **96**, 023422 (2017).

[76] S. Eckart, M. Kunitski, M. Richter, A. Hartung, J. Rist, F. Trinter, K. Fehre, N. Schlott, K. Henrichs, L. Ph.H. Schmidt, T. Jahnke, M. Schöffler, K. Liu, I. Barth, J. Kaushal, F. Morales, M. Ivanov, O. Smirnova, and R. Dörner, Nat. Phys. **14**, 701 (2018).

[77] K. Liu, H. Ni, K. Renziehausen, J.-M. Rost, and I. Barth, Phys. Rev. Lett. **121**, 203201 (2018).

[78] D. Trabert, A. Hartung, S. Eckart, F. Trinter, A. Kalinin, M. Schöffler, L. Ph.H. Schmidt, T. Jahnke, M. Kunitski, and R. Dörner, Phys. Rev. Lett. **120**, 043202 (2018).
[79] T. Nubbemeyer, K. Gorling, A. Saenz, U. Eichmann, and W. Sandner, Phys. Rev. Lett. **101**, 233001 (2008).
[80] U. Eichmann, A. Saenz, S. Eilzer, T. Nubbemeyer, and W. Sandner, Phys. Rev. Lett. **110**, 203002 (2013).
[81] M. Chini, X. Wang, Y. Cheng, H. Wang, Y. Wu, E. Cunningham, P.-C. Li, J. Heslar, D. A. Telnow, S.-I Chu, and Z. Chang, Nat. Photon. **8**, 437 (2014).
[82] H. Zimmermann, J. Buller, S. Eilzer, and U. Eichmann, Phys. Rev. Lett. **114**, 123003 (2015).
[83] R. R. Freeman, P. H. Bucksbaum, H. Milchberg, S. Darack, D. Schumacher, and M. E. Geusic, Phys. Rev. Lett. **59**, 1092 (1987).
[84] M. D. Perry, A. Szoke, and K. C. Kulander, Phys. Rev. Lett. **63**, 1058 (1989).
[85] P. Agostini, P. Breger, A. L'Huillier, H. G. Muller, G. Petite, A. Antonetti, and A. Migus, Phys. Rev. Lett. **63**, 2208 (1989).
[86] K. Krajewska, I. I. Fabrikant, and A. F. Starace, Phys. Rev. A **86**, 053410 (2012).
[87] Q. Li, X.-M. Tong, T. Morishita, H. Wei, and C. D. Lin, Phys. Rev. A **89**, 023421 (2014).
[88] Q. Li, X.-M. Tong, T. Morishita, C. Jin, H. Wei, and C. D. Lin, J. Phys. B **47**, 204019 (2014).
[89] W.-H. Xiong, J.-Z. Jin, L.-Y. Peng, and Q. Gong, Phys. Rev. A **96**, 023418 (2017).
[90] B. Piraux, F. Mota-Furtado, P. F. O'Mahony, A. Galstyan, and Yu. V. Popov, Phys. Rev. A **96**, 043403 (2017).
[91] J. Venzke, R. Reiff, Z. Xue, A. Jaron-Becker, and A. Becker, Phys. Rev. A **98**, 043434 (2018).
[92] E. Cormier and P. Lambropoulos, J. Phys. B **29**, 1667 (1996).
[93] Y. C. Han and L. B. Madsen, Phys. Rev. A **81**, 063430 (2010).
[94] H. R. Gray, R. M. Whitley, and C. R. Stroud, Opt. Lett. **3**, 218 (1978).
[95] M. V. Fedorov, M. M. Tehranchi, and S. M. Fedorov, J. Phys. B **29**, 2907 (1996).
[96] D. G. Arbo, K. I. Dimitriou, E. Persson, and J. Burgdörfer, Phys. Rev. A **78**, 013406 (2008).

Correction: The surname of the fourth author appeared incorrectly due to a database error and has been fixed.